CONF-791058--61

TOTAL-NEUTRON CROSS SECTIONS OF HEAVY NUCLEI

by

W.P. Poenitz, J.F. Whalen and A.B. Smith

MASTER

Prepared for

International Conference

Nuclear Cross Sections for Technology

Knoxville, Tennessee

October 22-26, 1979

U of C-AUA-USDOE

ARGONNE NATIONAL LABORATORY, ARGONNE, ILLINOIS

Operated under Contract W-31-109-Eng-38 for the

U. S. DEPARTMENT OF ENERGY

DISCLAIMER

TOTAL-NEUTRON CROSS SECTIONS OF HEAVY NUCLEI

W P. Poenitz, J. F. Whalen and A. B. Smith
Argonne National Laboratory
9700 South Cass Avenue
Argonne, Illinois 60439, USA

ABSTRACT

Total-neutron cross sections of the heavy and actinide nuclei ^{181}Ta, ^{197}Au, ^{232}Th, ^{233}U, ^{235}U, ^{238}U, ^{239}Pu and ^{240}Pu were measured from 30 keV to 4.8 MeV. The experimental procedures emphasized a high consistency of the measured data. Systematic uncertainties, excluding those associated with sample masses, were $\lesssim$0.5% and statistical uncertainties were typically $\leq$1.0%. At low energies attention was given to resonance self-shielding effects. The experimental results are in good agreement with ^{232}Th, ^{233}U and ^{238}U data previously reported from this laboratory and at higher energies with the comparable values reported by Foster and Glasgow[1], excepting ^{240}Pu which was not studied in the latter work. The measured total-cross-sections were interpreted in terms of a spherical optical model and a deformed coupled-channels model.

[Total neutron cross section, 0.03-4.8 MeV, ^{181}Ta, ^{197}An, ^{232}Th, ^{233}U, ^{235}U, ^{238}U, ^{239}Pu, ^{240}Pu.]

INTRODUCTION

The measurement of total-neutron cross sections is a straight forward task using conventional transmission techniques that are inherently self normalizing and employ relatively simple equipment. This is particularly so when, as in the present work, energy-averaged cross sections are determined. In the latter cases the total cross sections are deduced from the energy-average transmission of neutrons through the sample,

$$\langle T \rangle = \langle \exp(-n\sigma(E)) \rangle. \qquad (1)$$

However, fine energy-dependent structure may be present and then the average transmission yields the average cross section, $\langle\sigma\rangle$, only to the extent that the exponential of Eq. 1 can be approximated by the linear term, $1-n\sigma(E)$, at all energies. This implies samples that are sufficiently thin so that $n\sigma(E) \ll 1$ at all energies.

In view of the simplicity of techniques involved, it is surprising that large discrepancies and/or omissions persist in total-neutron-cross-section data.[2,3] The situation is further complicated by the frequent and erroneous interpretation of reported experimental total-neutron cross sections as "true" average total-neutron cross sections, $\langle\sigma\rangle$, when they are often "effective" average cross sections, σ_{eff}, obtained at room temperature for a specific sample thickness via the inversion of Eq. 1; i.e.,

$$\sigma_{eff} = \frac{-1}{n} \ln \langle T \rangle.$$

An improved knowledge of total-neutron cross sections of heavy nuclei is desirable for a number of technological reasons. Such data are the essential envelope of evaluated data sets to which the individual partial cross sections must conform. The potential accuracy of total-neutron cross sections often can guide the evaluation of partial cross sections. The total-neutron cross section is often one of the most unambiguous model-calculable quantities (e.g., using the optional model) and thus its precise provision can guide the choice of models essential for the extrapolation and interpolation of measured data in the actinide region where radioactivity and/or sample problems make explicit measurements difficult or even impossible. It was the objective of the present work to provide accurate and internally consistent total-neutron cross sections in the heavy and actinide region and to examine their systematics and the model implications.

MEASUREMENT TECHNIQUES AND METHODS

The measurements consisted of the determination of the average transmission of a collimated neutron beam through the heavy-nuclide samples. All the measurements employed fast-neutron time-of-flight techniques at the Argonne National Laboratory Fast Neutron Generator (FNG) in one of two modes. In the "monoenergetic" mode velocity spectra were interpreted to define the primary source and control background with the incident-neutron energy and resolution defined by the neutron source. In the second "pseudo-white" mode the incident neutron energy and resolution was determined from the measured neutron flight times and flight paths using a pseudo-white neutron source. In both modes the ^{7}Li(p,n) ^{7}Be reaction provided the pulsed neutron source with proton bursts of $\approx$ 1n sec at a repetition rate of 2MHz (monoenergetic) or 0.5 MHz (white). The monoenergetic mode was employed from $\approx$ 200 keV-to 4.8 MeV with incident-neutron energy spreads of 40-120 keV. At lower energies the white mode was used with a pseudo-white source-energy spread of $\approx$ 250 keV.

A shield and collimator placed about the neutron source defined a neutron beam at a zero-degree reaction angle having a diameter in the range $\approx$ 0.5 - 1.0 cm.

The Ta, Au, Th, ^{233}U, ^{235}U, ^{238}U, ^{239}Pu and ^{240}Pu measurement samples were all right-circular metallic cylinders with densities ranging from 0.067 at/b (Th) to 0.100 at/b (Ta). The actinide samples were isotopically enriched to between 93.18% (^{235}U) and 99.76% (^{233}U). The Ta, Au, Th and ^{238}U (i.e., U) samples were elemental. Highly active samples were canned in 0.025 cm thick stainless steel shells. Chemical inpurities were negligible. During measurement periods the samples were placed $\approx$ 160 cm from the neutron source, on the collimated beam axis and with neutrons incident on the cylinder bases.

Seven samples and a void (or empty can) were mounted on an eight position wheel which rotated at $\sim$ 3 rpm in a stepping manner alternately placing samples and void in the neutron beam. Eight time-of-flight spectra were obtained correlated with the sample and void positions of the wheel. Thus the cumulative spectra were a sum of a large number of individual short measurements made in rapid sequence. As a consequence any fluctuations of the source intensity were averaged out thus avoiding the conventional source monitor employed in the more usual sample-in, sample-out measurement technique. A number

of samples were referenced to the same void position, thereby increasing the efficiency of the system by nearly 50% relative to the usual "in-out" method. Since the samples see essentially identical source configurations improved measurement consistency can be expected.

A hydrogenous scintillation detector was used at energies above $\approx$ 1 MeV.[2] The detector was placed $\approx$ 780 cm from the source and associated pulse-shape-sensitive circuitry reduced the γ-ray sensitivity. At lower neutron energies, and extending up to $\approx$ 2 MeV, a "Black Neutron Detector" (BND)[4] was used. This device has a high low-energy efficiency with neutron detection down to $\approx$ 10 keV. However, statistical and background considerations set a lower-energy limit of 30-40 keV in the present measurements. A random-event pulser, time correlated with the pulsed-neutron source, was added to the detector signal.[5] This test pulse clearly determined the dead-time perturbations of the entire measurement system. These were usually < 1% and rarely exceeded 2%.

Data acquisition and processing was with an on-line computer system.[6] This system not only properly correlated samples and detector response but also processed the incoming information in "real time" so as to provide continuously updated total-cross-section results. This procedure not only improved the experimental efficiency but also provided for a continual monitoring of experimental progress.

Generally, measurements were made in two sample sets with Th, U and a carbon-reference sample common to both sets. Each set contained a void or empty stainless-steel container position, as appropriate, for the determination of the primary beam intensity. The carbon-reference sample provided a verification of system performance and established the energy scale and energy resolution using well known carbon resonances.[7] The carbon total cross sections resulting from the present measurements generally agreed with those of ENDF/B-V to within $\approx$ 0.5%.[7] Energy calibrations for the lower-energy "white" spectrum measurements were established by observation of well known neutron resonances in iron.[7]

DATA CORRECTIONS

Corrections associated with neutron inscattering, transmission through collimator walls and transmission through the air of the void, and for the isotopic composition of the samples were considered and found negligible. However, resonance self-shielding in the unresolved resonance region was a major concern. The samples were relatively large, therefore, the uncorrected experimental result is the effective, σ_{eff}, total-neutron cross section for the particular sample thickness at a nominal temperature of 293°K. The problem of resonance self-shielding in the unresolved resonance region is well known in the interpretation of neutron capture-cross-section measurements and is usually considered together with neutron-scattering perturbations. Analytical approximations for such corrections have been described by Schmitt,[8] Dresner,[9] and Macklin.[10] Similar corrections using Monte-Carlo techniques have been applied by Bogard and Semler,[11] Miller and Poenitz[12] and Froehner.[13] Detailed self-shielding attention has not been widely given to total-neutron cross sections despite the fact that the self-shielding effects can be large as illustrated, for example, in the context of structural materials, by Smith et al.[14] In the structural region a few very-high resolution results are available from which to determine quantitative self-shielding corrections. In the mass-energy region of the present work such high-resolution data does not exist and approximations used at lower energies[8-13] are not generally applicable. Simple model estimates indicate that self-shielding perturbations in the present context may exceed the experimental uncertainties even above 200 keV. The situation is illustrated by the ^{238}U example of Fig. 1. The potential cross section obtained from the hard-sphere model with $\ell \leq 4$, for example used by Froehner,[13] exceeds the total neutron cross section above $\approx$450 keV. The self-shielding effect should be sensitive to the differences between total and potential cross sections; i.e., to the fluctuating cross section, and is thus underestimated. Calculations using restricted angular momenta, $\ell \leq 2$, e.g. Miller and Poenitz[12]) and reactor codes (e.g., MC^{2}[15])are not much better as they tend to underestimate the potential scattering by only small amounts.

For the present work a Monte-Carlo self-shielding code was developed. It is based upon the single-level Breit-Wigner formulation of the resonances and a potential cross section derived from the optical model.

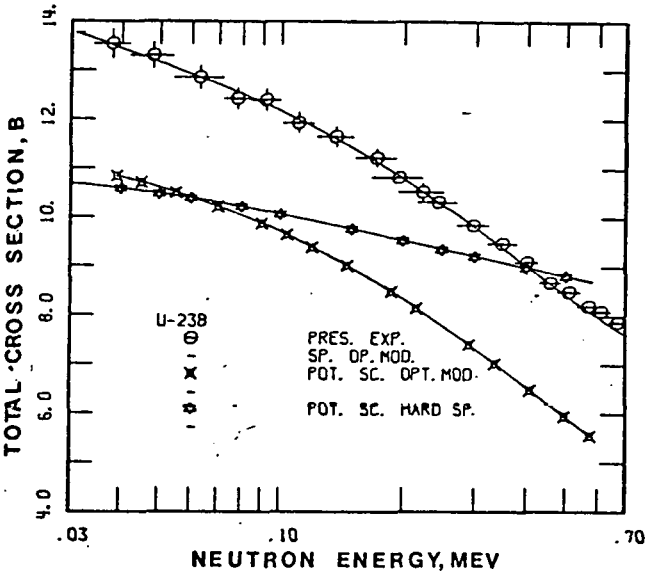

Fig. 1. Comparison of measured and calculated neutron total and potential-scattering cross sections of ^{238}U as discussed in Sec. III of the text.

The cross section is expressed as

$$\sigma_{tot} = \sigma_o \frac{1}{1+X^2} + \sigma_o \left(\frac{\sigma_{pot}}{\sigma_\chi}\right)^{1/2} \cdot \frac{2X}{1+X^2} + \sigma_{pot} \qquad (2)$$

where

$\sigma_o = \sigma_\chi g_J \Gamma_n/\Gamma$, $\sigma_\chi = 4\pi\chi^2$ and $X = 2(E-E_o)/\Gamma$.

Averaging over many resonances yields

$$\sigma_{tot} = \frac{\sigma_\chi}{4} \cdot \frac{2\pi g_J \overline{\Gamma}_n}{D_J} + \sigma_{pot}. \qquad (3)$$

Using the relationship

$$\frac{2\pi g_J \overline{\Gamma}_n}{D_J} = -\ell n \left(|\eta|^2\right), \qquad (4)$$

with $\eta = e^{-2i\delta}$, between the resonance parameters and the complex optical model phase shift, δ, as derived by Moldauer[16] one obtains

$$\sigma_{pot} = \frac{\sigma_\chi}{2}(1-\mathrm{Re}\eta + \frac{1}{2}\ell n(1-T)) = \sigma_{tot} + \frac{\sigma_\chi}{4}\ell n(1-T) \quad (5)$$

where $T = 1-|\eta|^2$ is the optical model transmission coefficient. The potential cross section derived from Eq. 5 is compared with measured and calculational values in Fig. 1.

Eqs. 4 and 5 were used to determine resonance parameters and potential cross sections for use in Eq. 1. Level spacings were calculated from the Fermi-gas model level density formula

$$\rho(E,J) = C \cdot (2J+1)\exp\left[-\frac{(2J+1)^2}{8\sigma^2}\right]\exp(2\sqrt{aE}) \quad (6)$$

where C is the constant for normalization to experimental values in the low eV range. The spin-cut-off factor, σ, and temperature constant, a, are discussed in the literature (e.g., see Refs. 17-19). A Wigner distribution was assumed for the level spacings and a Porter-Thomas distribution for the width fluctuation. An optical potential with a volume-imaginary term was used with parameters adjusted to give good representations of the total cross sections in the 20-300 keV range and of the low-energy potential scattering cross section. The calculation was inclusive of up to four inelastic scattering channels. Doppler broadening was taken into account using the ϕ and χ functions of Ref. 20 in Eq. 1 instead of $1/(1+X^2)$ and $2X/(1+X^2)$ terms.

The resulting calculated self-shielding corrections were small for ^{233}U and ^{235}U (<1% above 40 keV), of intermediate size for ^{239}Pu, ^{240}Pu and Th (<3-5% above 40 keV), and substantial for U, Au and Ta (<7-14% above 40 keV). The present correction for Au agrees very well in the 40-50 keV range with the results of calculations by Schneider and Froehner[21] for samples of similar thickness. The present results are also in good agreement with the sample-thickness dependence of transmissions of neutrons through Ta observed by Byoun and Block.[22]

RESULTS AND ANALYSIS

The results of the present measurements are outlined in Fig. 2. These values are corrected for self-shielding and these corrections, as noted above, can be substantial in some cases. Therefore these correction factors are a matter of continuing experimental and calculational study. The statistical uncertainties in the measured cross sections are typically 1% for Ta, Au, Th, ^{233}U, ^{235}U and U above 100 keV and 2% for ^{239}Pu and ^{240}Pu and for all samples below 100 keV. Uncertainties due to sample densities were estimated to be 0.5-1.0% excepting ^{240}Pu where the measured density was 78% that of the ^{239}Pu sample. The measured density of the ^{240}Pu sample was believed known to 1% but it was not possible to destroy the sample to verify its homogenity.

The present results are in very good agreement with U and ^{233}U values and in resonable agreement with Th results recently measured at this Laboratory.[23,3,2] Extensive comparisons with other previously reported values are not possible here. However, comparisons with the data of Foster and Glasgow[1] are of particular interest as these previously-reported results include all but one of the present samples, appear internally consistent and the energy range extends from well within that of the present measurements to much higher energies of particular interest from the point of view of model derivations. The Foster and Glasgow data are also shown in Fig. 2. In these comparisons averages of the results of Ref. 1 are used consisting of ten values at the lower energies, decreasing to four at the highest energies. The agreement between the two sets of data for Au, ^{233}U, ^{235}U, U and ^{239}Pu is generally good, e.g., better than 1%, in the medium-range of overlap. There is some tendency for the data of Ref. 1 to be slightly lower at low energies and the present values tend to scatter more at their higher-energy extreme. The Ta and Th results of Ref. 1 appear to differ in normalization from those of the present work by ≈1-3%.

It is well known that a deformed optical model is more suitable for the description of many features of the neutron interaction with strongly deformed targets than is the simple spherical optical model. This is expected to be true of the representation of the total-neutron cross section although that cross section is not as sensitive to the details of the interaction as some of the partial cross sections. It has been shown, e.g., by Glasgow and Foster,[24] that global-spherical-optical potentials are not particularly suitable for describing the total-neutron cross sections in regions of strong deformation. Much improved descriptions in these regions have been obtained using couupled-channels models, e.g., Zuffi,[25] Madland and Young.[26]

Seven of the eight nuclei studied in the present work are strongly deformed with similar deformations, β, varying from 0.248(Th) to 0.287(^{233}U).[27] A model suitable for the description of the relevant total-neutron cross sections was sought based upon the present measured data, extended to higher energies using the results of Foster and Glasgow[1]; i.e., the data base shown in Fig. 2. Initially, spherical-optical-model parameters were chosen by a simultaneous fit to the experimental total-neutron cross sections of Ta, ^{233}U, ^{235}U, U and ^{239}Pu. The resulting potential parameters are given in Table I. The total-neutron cross sections of the remaining three nuclei were then calculated in a straightforward manner using the derived potential parameters. The spherical-potential parameters of Table I are rather conventional. The absorption is somewhat outside the mean real radius as often suggested[28] and the magnitude of the parameters are similar to those frequently reported in the literature. An exception is the rather narrow and deep surface absorption term but its effective strength, W·a, is again relatively conventional. The results obtained with this spherical potential, shown in Figs. 2 and 3, are in good agreement with the measured values excepting those for Au. The latter exception is expected as the spherical potential is a parameterization of total-neutron cross sections in a deformed nuclear region and should not be suitable for the spherical exception, Au.

Recently, Guenther, et al.,[29] have deduced a coupled-channels model for the description of the neutron interaction with ^{238}U giving particular attention to neutron scattering processes. This model was used to calculate total-neutron cross sections of Th and ^{240}Pu including the consideration of deformation with the results shown in Figs. 2 and 3.[30] Fig. 3 also shows a ^{240}Pu result obtained with the coupled-channels model of LaGrange and Jary.[31] The description of the total-neutron cross sections obtained with the coupled-channels model is marginally better than that obtained with the above simple spherical optical parameterization. The coupled-channels model is far more suitable when dealing with some of the partial-neutron-reaction channels (particularly scattering)[29] and consideration of these same partial reaction channels might well alter the above choice of a

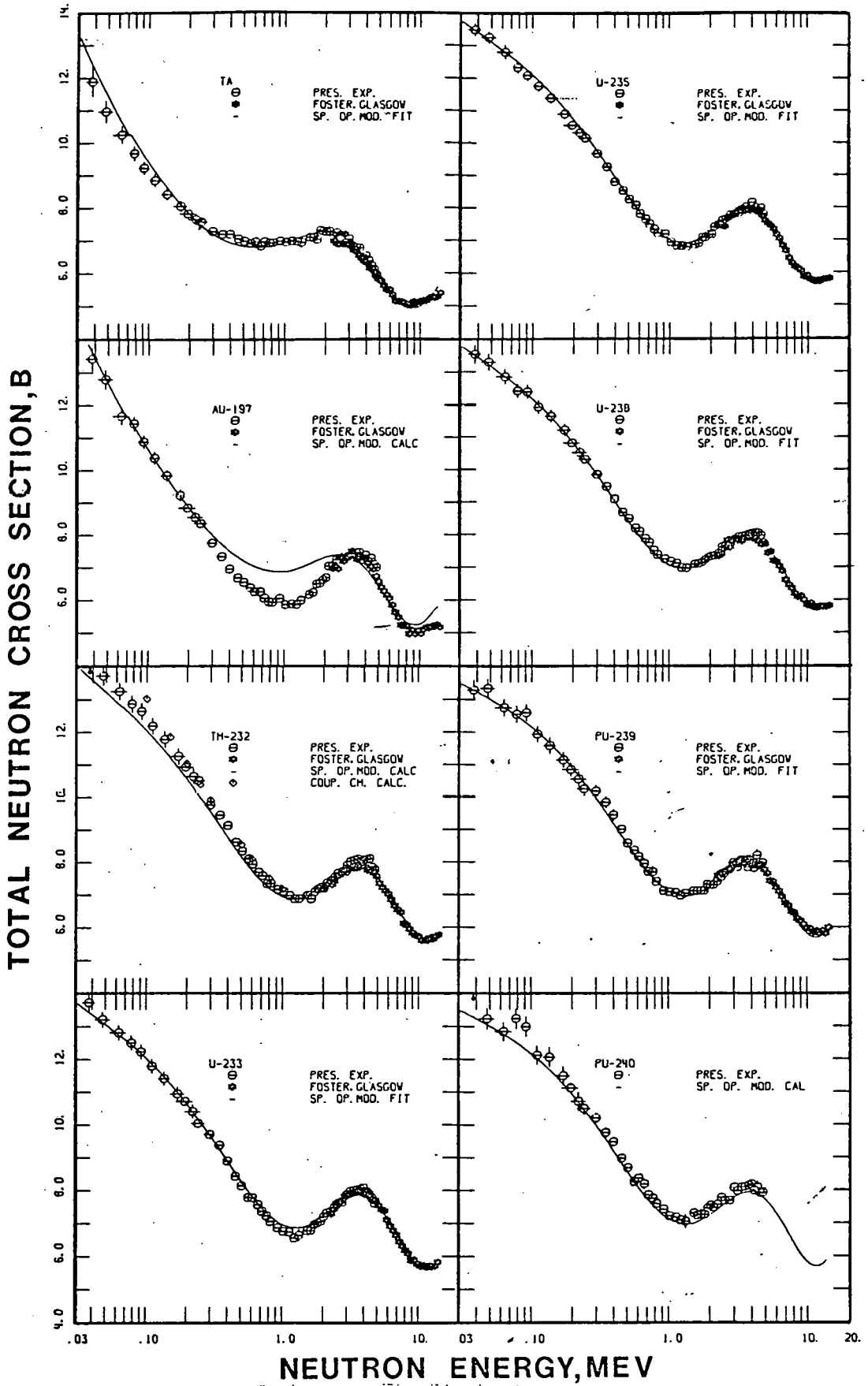

FIGURE 2.

Measured and calculated total-neutron cross sections of Ta, Au, Th, ^{233}U, ^{235}U, U, ^{239}Pu and ^{240}Pu. The present measured values are indicated by circular data points, those of Ref. 1 by star-shaped data points. Curves indicated the results of spherical and deformed optical-model calculations as outlined in Sec. IV of the text.

spherical parameterization. In addition, a properly chosen coupled-channels model has the desirable capability of concurrently treating both spherical nuclei and nuclei of various deformation not a characteristic of the spherical parameterization as illustrated by the above Au total-neutron cross sections.

TABLE I. Spherical-Optical-Potential Parameters[a]

Real Potential[b]

$$V = \underline{45.308} - \underline{0.100}\,E(MeV) - 24.0\,(N-Z)/A,\ MeV$$

$$R = \underline{1.285}\,A^{1/3} + 0.3,F$$

$$a = \underline{0.467},F$$

Imaginary Potential[c]

$$W = \underline{26.245} + \underline{0.427}\,E(MeV) - 12.0\,(N-Z)/A,\ MeV$$

$$R = \underline{1.403}\,A^{1/3} + 0.3,F$$

$$a = \underline{0.131},F$$

Spin-orbit Potential[d]

$$V_{so} = 7.0,\ MeV$$

[a] Underlined quantities were determined from fitting procedures.

[b] Saxon form.

[c] Saxon derivative form.

[d] Thomas form.

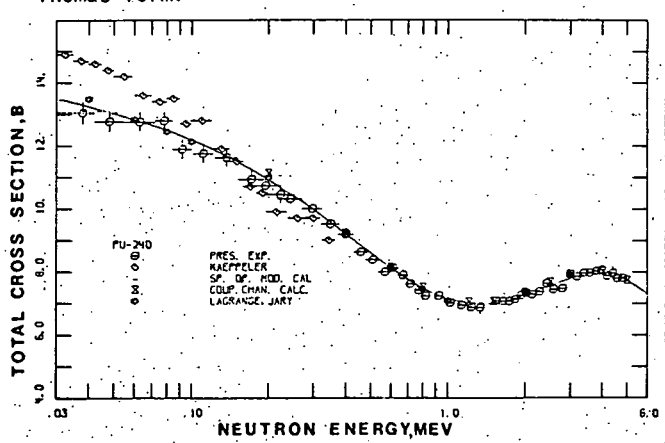

Fig. 3. Measured and calculated total-neutron cross sections of ^{240}Pu. The present measured values are indicated by circular data points. Other symbols and the curve denote the results of calculations as described in Sec. IV of the text.

The present experimental results give new definition to the total-neutron cross sections in a technologically important mass-energy region with particular attention to measurement accuracy, consistency of measured values and the effect of often ignored and frequently substantial self-shielding corrections. The result is a precise total-neutron cross section data base that should bring improved accuracies to important evaluations and better definition to theoretical models.

ACKNOWLEDGEMENTS

The authors greatly acknowledge the consultation and advice of Dr. P. A. Moldauer during the course of this work. The work is supported by the U. S. Department of Energy.

REFERENCES

1. D. Foster and D. Glasgow, Phys. Rev., C3 576 (1971).
2. J. Whalen and A. Smith, Nucl. Sci. and Eng., 67 129 (1978).
3. W. P. Poenitz et al., Nucl. Sci. and Eng., 68 358 (1978).
4. W. P. Poenitz, Argonne National Laboratory Report, ANL-7915 (1978).
5. W. P. Poenitz, Argonne National Laboratory Report, ANL/NDM-36 (1978).
6. W. P. Poenitz and J. F. Whalen, Argonne National Laboratory Report, ANL-8026 (1973).
7. C. Fu and F. Perey, Atomic and Nucl. Data Tables, 22 249 (1978). See also ENDF/B-IV for both carbon and iron reference values.
8. H. W. Schmitt, Oak Ridge National Laboratory Report, ORNL-2883 (1960).
9. L. Dresner, Nucl. Instr. and Methods, 16 176 (1962).
10. R. L. Macklin, Nucl. Instr. and Methods, 26 213 (1964).
11. D. Bogard and T. Semler, Conf. on Neutron Cross Sections and Technology, CONF-660303, 502, Vol. -1 (1966).
12. L. B. Miller and W. P. Poenitz, Nucl. Sci. and Eng., 35 295 (1969).
13. F. H. Froehner, Gulf-General Atomic Report GA-8380 (1968).
14. A. Smith et al., Fast-neutron Total and Scattering Cross Sections of Cr, Fe and ^{60}Ni; NEANDC Topical Conference, Geel (1979).
15. H. Henryson and B. Toppel, Argonne National Laboratory Report, ANL-8144 (1976).
16. P. A. Moldauer, Phys. Rev. Lett. 177 1841 (1976).
17. A. V. Malyshew, Soviet Physics, JETP; 18 221 (1964).
18. N. Abdelmalec and V. Stravinsky, Nucl. Phys, 58 601 (1964).
19. J. E. Lynn, Atomic Energy Research Estabishment Report, AERE-R7468 (1974).
20. L. Dresner, Resonance Absorption in Nuclear Reactors, Pergamon Press, New York (1960).
21. E. Schneider and F. Froehner, Conf. on Nuclear Data for Reactors, Vol. -1,201 (1970) Helsinki; Proc. pub. by IAEA press.
22. T. Byoun and R. Block, Conf. on Neutron Cross Sections and Technology, CONF-710301, Vol. -II, 895 (1971).
23. W. P. Poenitz, et al., Argonne National Laboratory Report, ANL/NDM-32 (1977); also private communication from A. Smith with data available at the National Nuclear Data Center, Brookhaven National Laboratory (1978).
24. D. Glasgow and D. Foster, Phys. Rev., C3 604 (1971).
25. L. Zuffi, Nucl. Sci. and Eng., 68 357 (1978).
26. D. Madland and P. Young, Proc. Conf. on Nuclear Data for Reactors and Other Applications, Harwell (1978).
27. Nuclear Data Tables, A7 495 (1970).
28. P. A. Moldauer, Nucl. Phys., 47 656 (1963).
29. P. Guenther et. al., Argonne National Laboratory Report, ANL/NDM-16 (1975).
30. All coupled-channel calculations were carried out with the computer code JUPREX, P. A. Moldauer, private-communication (1979).
31. C. LaGrange and J. Jary, INDC Report, INDC (FR) -30/L (1978).